

## Supplementary file

# Identification of gedunin from a phytochemical depository as a novel multidrug resistance-bypassing tubulin inhibitor of cancer cells

Sami A. Khalid<sup>1,\*</sup>, Mona Dawood<sup>2,4</sup>, Joelle C. Boulos<sup>2</sup>, Monica Wasfi<sup>1</sup>, Assia Drif<sup>2</sup>, Mohamed E. M. Saeed<sup>2</sup>, Faranak Bahramimehr<sup>2</sup>, Nasim Shahhamzehei<sup>2</sup>, Letian Shan<sup>3</sup>, Thomas Efferth<sup>2,\*</sup>

<sup>1</sup> Faculty of Pharmacy, University of Science & Technology, Omdurman, Sudan

<sup>2</sup> Department of Pharmaceutical Biology, Institute of Pharmaceutical and Biomedical Sciences, Johannes Gutenberg University, Staudinger Weg 5, 55128 Mainz, Germany

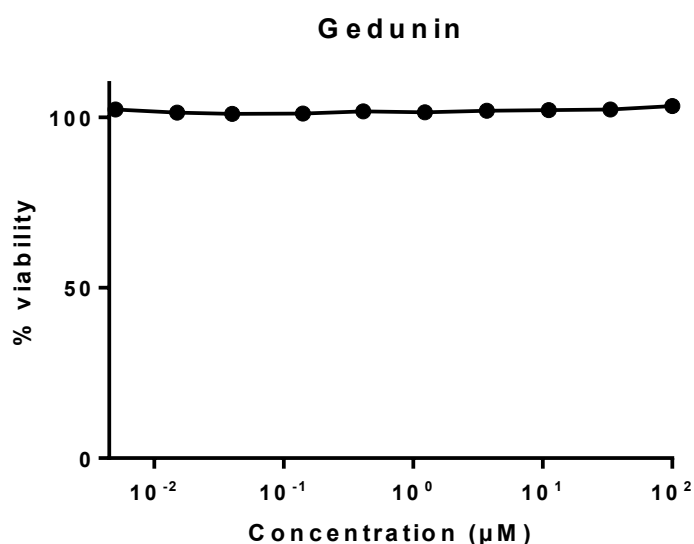
<sup>3</sup> The First Affiliated Hospital, Zhejiang Chinese Medical University, Hangzhou, 310053, Zhejiang, China

<sup>4</sup> Home address: Department of Molecular Biology, Faculty of Medical Laboratory Sciences, Al-Neelain University, Khartoum, Sudan

\* Correspondence:

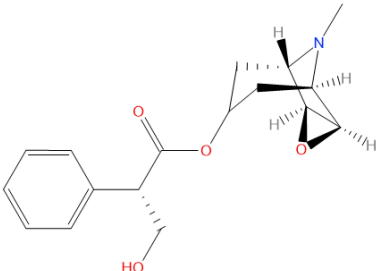
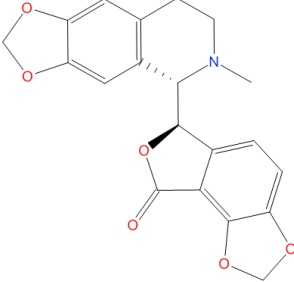
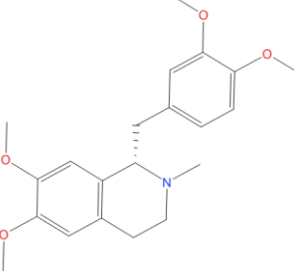
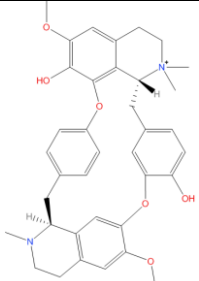
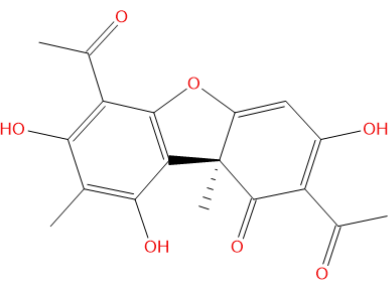
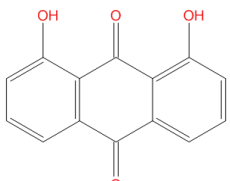
S. Khalid (E-mail: khalidseek@hotmail.com)

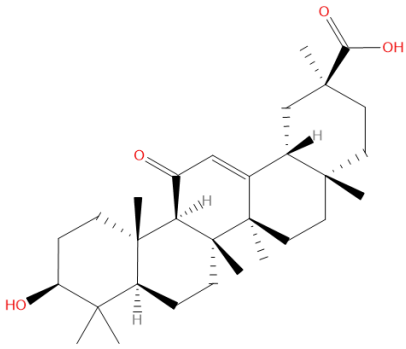
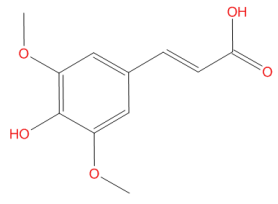
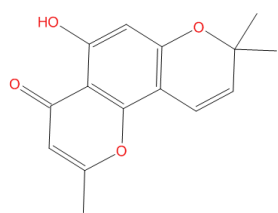
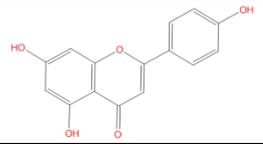
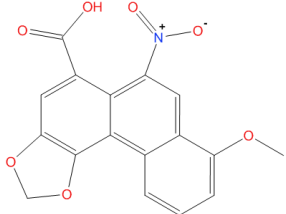
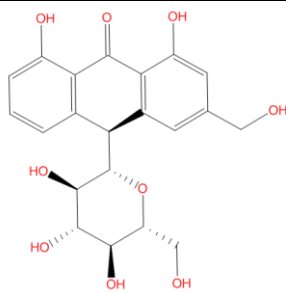
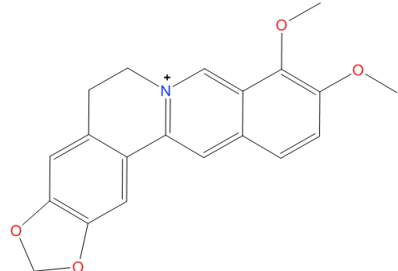
T. Efferth (E-mail: efferth@uni-mainz.de)

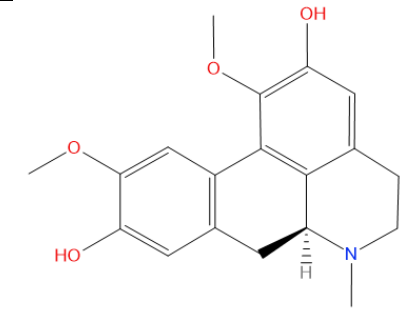
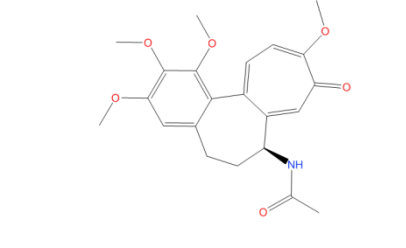
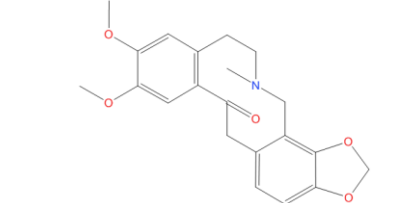
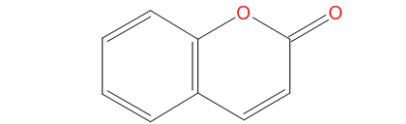
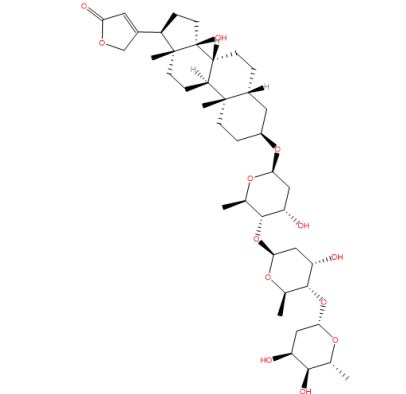
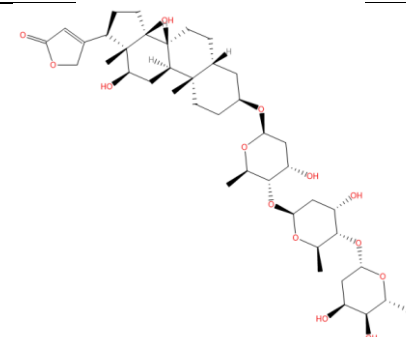


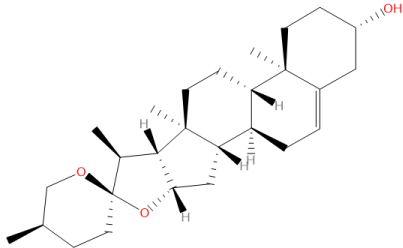
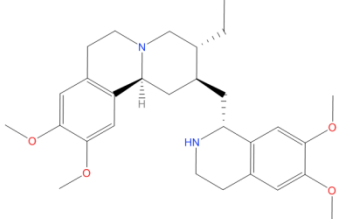
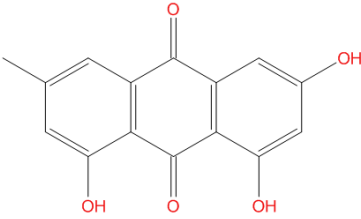
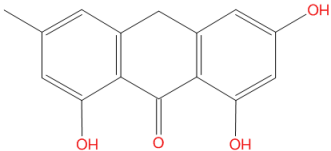
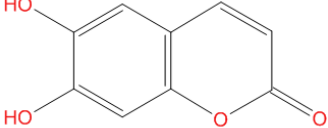
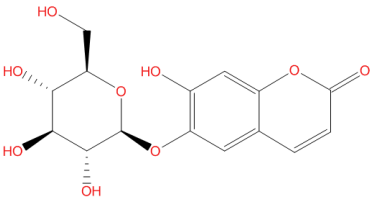
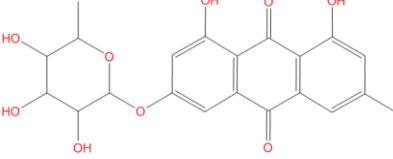
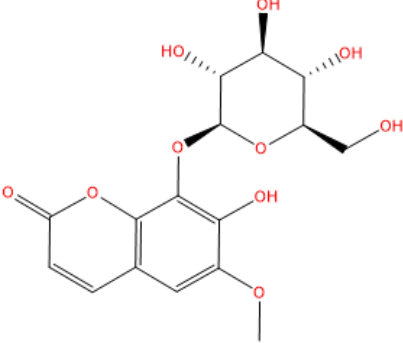
**Supplementary Figure S1:** Cytotoxicity of Gedunin on PBMCs. Each point illustrates the mean value  $\pm$  SD of two independent experiments with six replicates each.

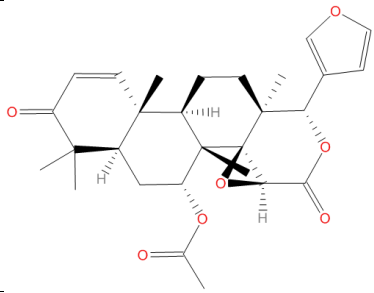
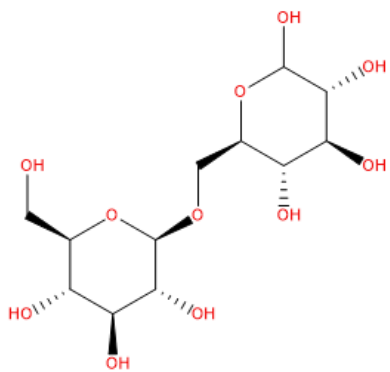
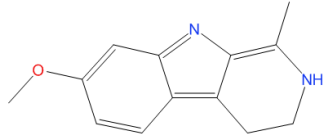
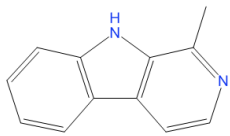
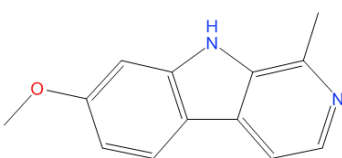
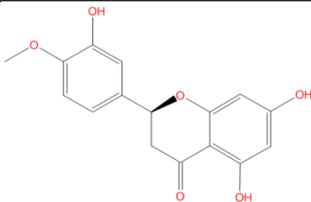
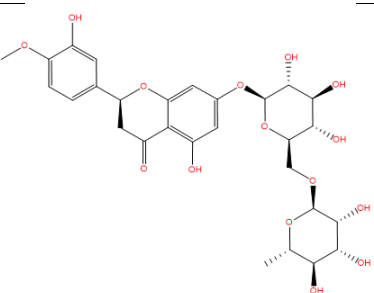
**Supplementary Table SI:** Characteristics of phytochemicals with SAK-T code.

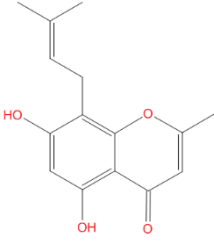
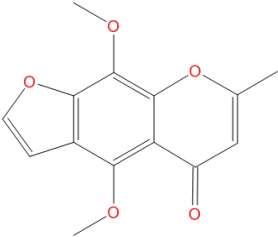
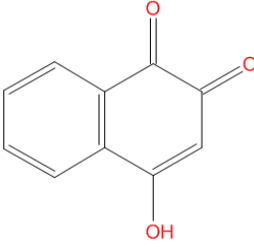
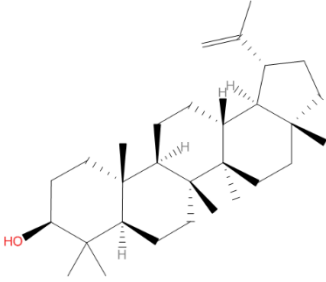
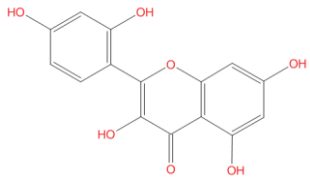
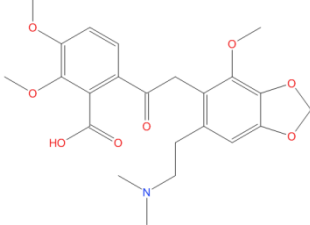
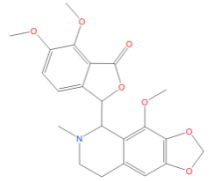
Code	Compound	MW	CID Code	2D Structure
SAK-T1	(-)-Scopolamine hydrochloride	339.82	6852406	 The structure shows a tropane bicyclic core (8-azabicyclo[3.2.1]octane) with a methyl group on the nitrogen. It is linked via an ester bond to a propyl chain, which is further substituted with a phenyl ring and a hydroxyl group.
SAK-T2	(+)-Bicuculline	367.35	10237	 The structure features a tropane bicyclic core with a methyl group on the nitrogen. It is substituted with a 2,3-dihydrobenzofuran ring system and a 2,3-dihydroisobenzofuran ring system.
SAK-T3	(+)-Laudanosine	357.45	73397	 The structure shows a tropane bicyclic core with a methyl group on the nitrogen. It is substituted with a 3,4,5-trimethoxyphenyl ring and a 2,4,6-trimethoxyphenyl ring.
SAK-T4	(+)-Tubocurarine	609.74	6000	 The structure is a complex dimeric alkaloid consisting of two tropane bicyclic cores linked together. It features multiple methoxy and hydroxyl groups on the aromatic rings.
SAK-T5	(+)-Usnic acid	344.31	442614	 The structure is a dimeric phenol with a central ether bridge. It has multiple hydroxyl and acetyl groups on the aromatic rings.
SAK-T6	1,8-Dihydroxyanthraquinone	240.21	2950	 The structure is a linear anthraquinone with hydroxyl groups at the 1 and 8 positions.

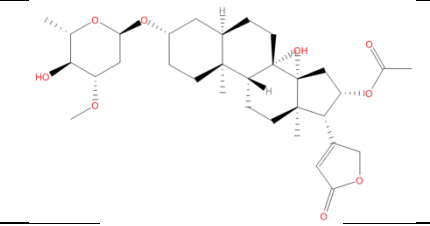
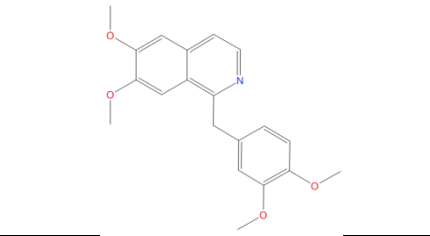
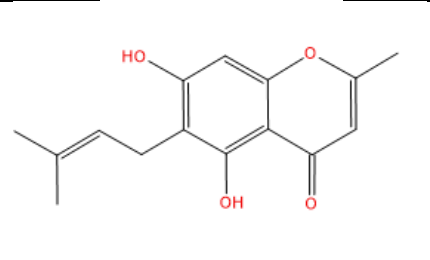
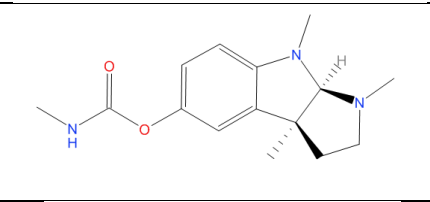
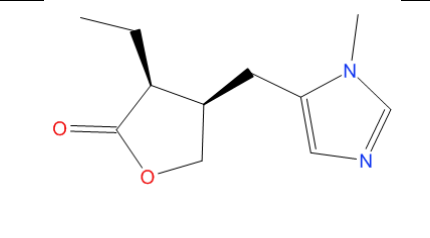
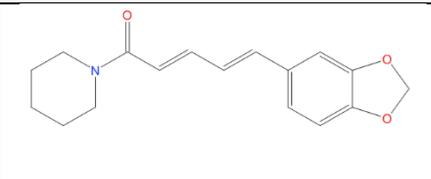
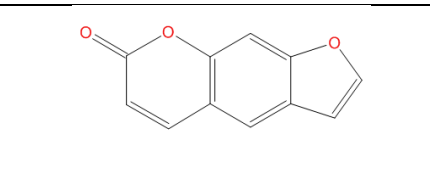
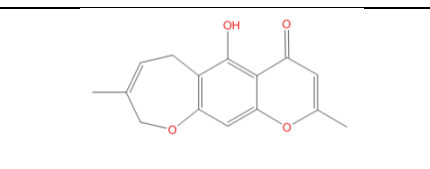
SAK-T7	18-beta-Glycyrrhetic acid	470.69	10114	
SAK-T8	3,5-Dimethoxy-4-hydroxycinnamic acid	224.21	637775	
SAK-T9	Alloptaeroxylin	258.27	12305984	
SAK-T10	Apigenin	270.24	5280443	
SAK-T11	Aristolochic acid	341.27	2236	
SAK-T12	Barbaloin	418.398	12305761	
SAK-T13	Berberine	371.81	2353	

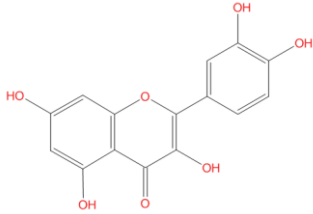
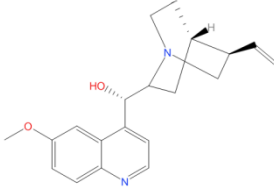
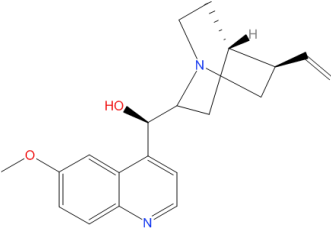
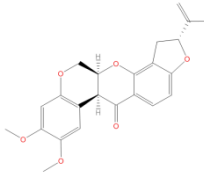
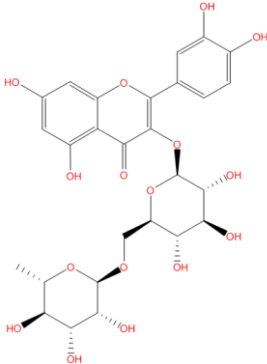
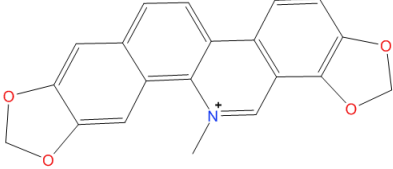
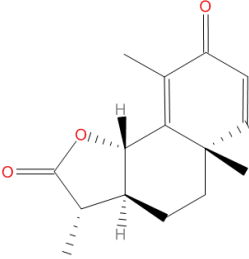
SAK-T14	Boldine	327.38	10154	
SAK-T15	Colchicine	399.44	6167	
SAK-T16	Cryptopine	369.41	72616	
SAK-T17	Cumarin	146.14	323	
SAK-T18	Digitoxin	764.95	441207	
SAK-T19	Digoxin	780.94	2724385	

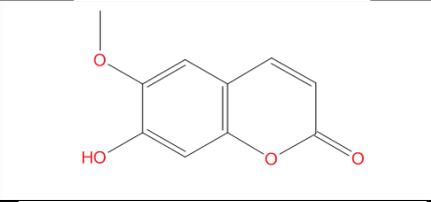
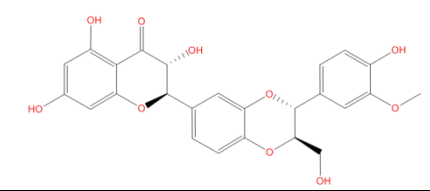
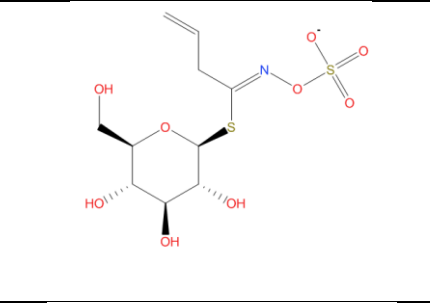
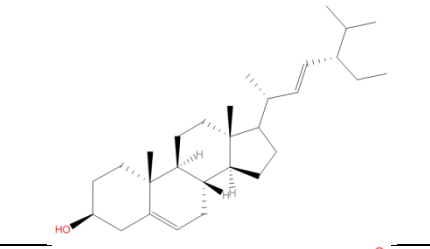
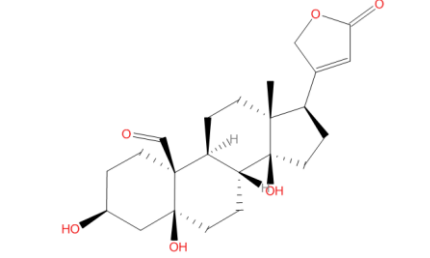
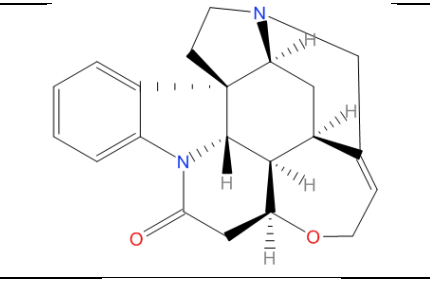
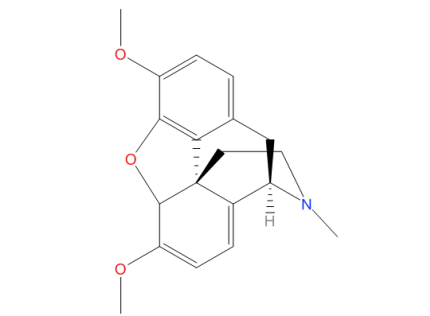
SAK-T20	Diosgenin	414.63	99474	
SAK-T21	Emetine dihydrochloride	553.56	3068143	
SAK-T22	Emodin	270.24	3220	
SAK-T23	Emodin anthrone	256.26	122635	
SAK-T25	Esculetin	178.14	5281416	
SAK-T26	Esculin	340.28	5281417	
SAK-T27	Frangulin	416.37	348160	
SAK-T28	Fraxin	370.31	5273568	

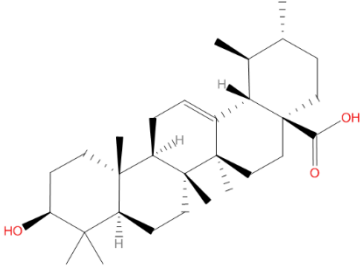
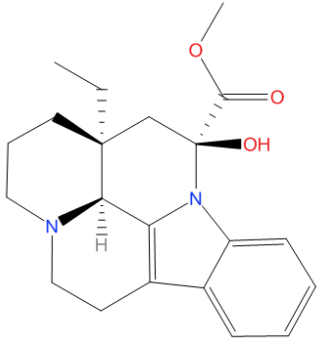
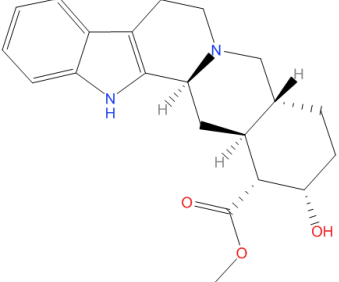
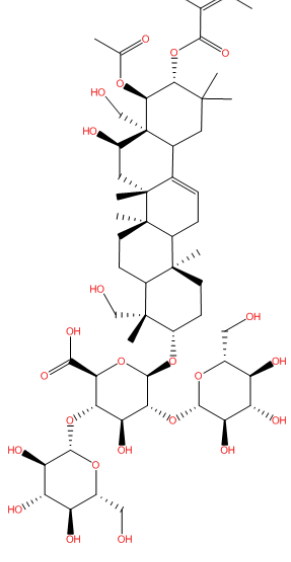
SAK-T29	Gedunine	482.57	12004512	
SAK-T30	Gentibiose	342.30	5460026	
SAK-T31	Harmaline	214.26	3564	
SAK-T32	Harman	182.22	5281404	
SAK-T33	Harmine	212.25	5280953	
SAK-T34	Hesperetin	302.282	72281	
SAK-T35	Hesperidin	610.57	10621	

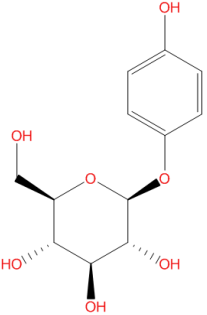
SAK-T36	Heteropeucenin	260.29	12310443	
SAK-T37	Khellin	260.24	3828	
SAK-T38	Lawsone	174.15	6755	
SAK-T39	Lupeol	426.72	259846	
SAK-T40	Morin	302.24	5281670	
SAK-T41	Narceine	445.47	8564	
SAK-T42	Narcotine	413.42	4544	

SAK-T43	Oleandrin	576.72	11541511	
SAK-T45	Papaverine	375.85	6084	
SAK-T46	Peucenin, (5,7-dihydroxy-6-isopentyl-2-methylchromone)	274.12	68477	
SAK-T47	Physostigmine	275.35	5983	
SAK-T48	Pilocarpine	208.26	5910	
SAK-T49	Piperine	285.34	638024	
SAK-T50	Psoralen	186.16	6199	
SAK-T51	Ptaeroxylin	258.27	3646533	

SAK-T52	Quercetin dihydrate	338.27	5280343	
SAK-T53	Quinidine	324.42	441074	
SAK-T54	Quinine sulphate	782.96	16211610	
SAK-T55	Rotenone	394.42	6758	
SAK-T58	Rutin	610.52	5280805	
SAK-T59	Sanguinarine	367.78	68635	
SAK-T60	Santonin	246.30	221071	

SAK-T61	Scopoletine	192.17	5280460	
SAK-T62	Silibinin	482.441	31553	
SAK-T63	Sinigrin monohydrate	415.47	23670774	
SAK-T64	Stigmasterol	412.69	5280794	
SAK-T65	Strophanthidin	404.5	6185	
SAK-T66	Strychnine	334.42	441071	
SAK-T67	Thebaine alkaloid	311.38	5321926	

SAK-T68	Ursolic acid	456.71	64945	
SAK-T69	Vincamine	354.44	15376	
SAK-T70	Yohimbine hydrochloride	390.91	6169	
SAK-T71	$\beta$ -Escin	1131.26	6540709	

SAK-T72	P-Arbutin	272.25	440936	 <p>The image shows the chemical structure of P-Arbutin, which is a cyclic hemiacetal. It consists of a six-membered ring with an oxygen atom at the top position. The ring carbons are substituted with hydroxyl groups: C2 has a hydroxyl group on a wedge, C3 has a hydroxyl group on a dash, C4 has a hydroxyl group on a wedge, and C5 has a hydroxyl group on a dash. Attached to the ring oxygen is a 4-hydroxyphenyl group, represented as a benzene ring with a hydroxyl group at the para position.</p>
---------	-----------	--------	--------	---

**Supplementary Table S2.** Pearson correlation test-based COMPARE analysis of proteins directly or inversely correlating with the  $\log_{10}IC_{50}$  values of gedunin in 55 tumor cell lines. The protein functions have been extracted from the GeneCards database (<https://www.genecards.org>).

Symbol	<i>r</i> -Value	<i>p</i> -Value	Entry Gene ID	Name	Function
<b>MOGS</b>	0.474	$1.28 \times 10^{-4}$	7841	Mannosyl-oligosaccharide glucosidase	Cleavage of glucose from oligosaccharide precursor
<b>PDS5A</b>	0.454	$2.51 \times 10^{-4}$	23244	PDS5 cohesin-associated factor A	Regulation of sister chromatid cohesion during mitosis
<b>IKBKAP</b>	0.438	$4.15 \times 10^{-4}$	8518	Elongator acetyltransferase complex subunit 1	Binding of NF- $\kappa$ B-inducing kinase and I- $\kappa$ B kinases to active the kinase complex
<b>SLC12A4</b>	0.432	$4.90 \times 10^{-4}$	6560	Solute carrier family 12 member 4	Coupled movement of potassium and chloride ions across the plasma membrane
<b>SPECC1</b>	0.425	$6.17 \times 10^{-4}$	92521	Sperm antigen with calponin homology and coiled-coil domains 1	May cause juvenile myelomonocytic leukemia.
<b>GDF15</b>	0.419	$7.22 \times 10^{-4}$	9518	Growth differentiation factor 15	Binding of TGF- $\beta$ receptors leads to the recruitment and activation of SMAD family transcription factors for gene expression. Involved in the stress response program of cells after cellular injury
<b>NUDC</b>	0.402	$1.16 \times 10^{-3}$	10726	Nuclear distribution C, dynein complex regulator	Spindle formation in mitosis and microtubule organization during cytokinesis.
<b>PA2G4</b>	0.397	$1.32 \times 10^{-3}$	5036	Proliferation-associated 2G4	Ribosome assembly and regulation of rRNA processing. Transcriptional co-repressor of cell cycle genes by interacting with histone deacetylases. Implicated in growth inhibition and differentiation of cancer cells
<b>IMPDH2</b>	0.386	$1.78 \times 10^{-3}$	3615	Inosine monophosphate dehydrogenase 2	De novo guanine nucleotide biosynthesis for DNA and RNA synthesis. Role in malignant transformation
<b>RPS28</b>	0.384	$1.88 \times 10^{-3}$	6234	Ribosomal protein S28	Involved in ribosomal protein synthesis
<b>PEA15</b>	0.377	$2.27 \times 10^{-3}$	8682	Proliferation and apoptosis adaptor protein 15	Negative apoptosis regulator.
<b>REEP5</b>	0.376	$2.35 \times 10^{-3}$	7905	Receptor accessory protein 5	Involved in endoplasmic reticulum organization and regulation of intracellular transport
<b>HM13</b>	0.374	$2.43 \times 10^{-3}$	81502	Histocompatibility minor 13	Intramembrane proteolysis of signal peptides
<b>PGRMC1</b>	0.366	$2.96 \times 10^{-3}$	10857	Progesterone receptor membrane component 1	Putative membrane-associated progesterone steroid receptor

<b>B2M</b>	0.365	$3.08 \times 10^{-3}$	567	$\beta$ -2-Microglobulin	Serum protein associated with the major histocompatibility complex (MHC) class I heavy chain
<b>AQR</b>	0.365	$3.09 \times 10^{-3}$	9716	Aquarius intron-binding spliceosomal factor	Involved in mRNA splicing via spliceosome
<b>HNRNPC</b>	0.364	$3.17 \times 10^{-3}$	3183	Heterogeneous nuclear ribonucleoprotein C	RNA-binding protein influencing pre-mRNA processing
<b>PSMA7</b>	0.359	$3.55 \times 10^{-3}$	5688	Proteasome 20S subunit $\alpha$ 7	Part of the 26S proteasome. Role in the cellular stress response by regulating hypoxia-inducible factor-1 $\alpha$
<b>EIF3G</b>	0.359	$3.57 \times 10^{-3}$	8666	Eukaryotic translation initiation factor 3 subunit G	Initiation of protein translation
<b>TRAP1</b>	0.358	$3.67 \times 10^{-3}$	10131	Tumor necrosis factor type 1 receptor-associated protein 1	Mitochondrial chaperone and member of the heat shock protein 90 (HSP90) family. Regulator of cellular stress responses
<b>DDX21</b>	-0.483	$9.22 \times 10^{-5}$	9188	DEAD (Asp-Glu-Ala-Asp) box helicase 21	Putative RNA helicase implicated in alterations of the RNA secondary structure. Involved in cellular growth and division
<b>MSH2</b>	-0.475	$1.25 \times 10^{-4}$	4436	MutS ( <i>E. coli</i> ) homolog 2 (colon cancer, nonpolyposis type 1)	Mismatch repair gene mutS
<b>UBE2S</b>	-0.469	$1.54 \times 10^{-4}$	27338	Ubiquitin conjugating enzyme E2 S	Ubiquitin-conjugating enzyme and ubiquitin carrier protein
<b>DRG1</b>	-0.460	$2.05 \times 10^{-4}$	4733	Developmentally regulated GTP binding protein 1	Positive regulation of microtubule polymerization and mitotic spindle assembly
<b>EIF3I</b>	-0.457	$2.25 \times 10^{-4}$	8668	Eukaryotic translation initiation factor 3 subunit I	Involved in translational initiation
<b>NEBL</b>	-0.453	$2.61 \times 10^{-4}$	10529	Nebulette	Binding of actin and interaction with thin filaments and Z-line-associated proteins in striated muscle
<b>EIF3E</b>	-0.454	$2.52 \times 10^{-4}$	3646	Eukaryotic translation initiation factor 3 subunit E	Positive regulation of mRNA binding activity, gene expression, and translational initiation
<b>CARM1</b>	-0.453	$2.54 \times 10^{-4}$	10498	Coactivator-associated arginine methyltransferase 1	Methylation of histones and other chromatin-associated proteins. Regulation of gene expression
<b>PPP2R1B</b>	-0.452	$2.66 \times 10^{-4}$	5519	Protein phosphatase 2 (formerly 2A), regulatory subunit A (PR 65), $\beta$ isoform	Ser/Thr phosphatase implicated in the negative control of cell growth and division
<b>AP2A1</b>	-0.450	$2.80 \times 10^{-4}$	160	Adaptor-related protein complex 2 subunit $\alpha$ 1	Component of the adaptor protein complex 2 (AP-2). Protein transport via transport vesicles in different membrane traffic pathways

<b>SEC22B</b>	-0.448	$2.97 \times 10^{-4}$	9554	SEC22 vesicle trafficking protein homolog B ( <i>S. cerevisiae</i> )	Endoplasmic reticulum to Golgi protein trafficking
<b>YIPF5</b>	-0.447	$3.15 \times 10^{-4}$	81555	Yip1 domain family member 5	Regulation of endoplasmic reticulum to Golgi vesicle-mediated transport
<b>ITGAV</b>	-0.446	$3.22 \times 10^{-4}$	3685	Integrin, Alpha V (vitronectin receptor, $\alpha$ polypeptide, antigen CD51)	Cell surface adhesion and signaling. Regulation of angiogenesis and cancer progression
<b>ABCD3</b>	-0.445	$3.30 \times 10^{-4}$	5825	ATP-binding cassette subfamily D member 3	Role in peroxisome biogenesis by fatty acid transport
<b>GNAI3</b>	-0.445	$3.31 \times 10^{-4}$	2773	Guanine nucleotide-binding protein G(I) subunit $\alpha$ -3	Transmembrane signal transduction.
<b>MBOAT7</b>	-0.443	$3.51 \times 10^{-4}$	79143	Membrane-bound O-acyltransferase domain-containing 7	Membrane-bound O-acyltransferase domain-containing 7
<b>GNAI1</b>	-0.440	$3.86 \times 10^{-4}$	2770	Guanine nucleotide-binding protein G(I) subunit $\alpha$ 1	Signal transduction of $\beta$ -adrenergic signals by inhibiting adenylate cyclase
<b>MMGT1</b>	-0.438	$4.11 \times 10^{-4}$	93380	Membrane magnesium transporter 1	Membrane insertase activity for endoplasmic reticulum proteins
<b>EIF3H</b>	-0.438	$4.16 \times 10^{-4}$	8667	Eukaryotic translation initiation factor 3 subunit H	Deubiquitinase and translation initiation factor activities. Implicated in breast, prostate, and prostate carcinoma
<b>FAF2</b>	-0.436	$4.38 \times 10^{-4}$	91942	Fas-associated factor family member 2	Apoptosis resistance to apoptosis in T cells and eosinophils